New pose estimation scheme in perspective vision system during civil aircraft landing

Victor Gibert, Laurent Burlion, Abdelhamid Chriette, Josep Boada, Franck Plestan

New pose estimation scheme in perspective vision system during civil aircraft landing

Victor GIBERT [*,***] **Laurent BURLION** [**] **Abdelhamid CHRIETTE** [***]
Josep BOADA [*] **Franck PLESTAN** [***]

[*] *Airbus Operations S.A.S., Toulouse, France (e-mail: victor.gibert@airbus.com, josep.boada-bauxell@airbus.com)*
[**] *ONERA, the French Aerospace Lab, 31055, Toulouse, France. (e-mail: laurent.burlion@onera.fr)*
[***] *LUNAM Université, Ecole Centrale de Nantes-IRCCyN, Nantes, France (e-mail: Abdelhamid.Chriette@irccyn.ec-nantes.fr, Franck.Plestan@irccyn.ec-nantes.fr)*

Abstract: In this paper, a new pose estimation solution for perspective vision system is presented and applied to a civil aircraft landing phase. Vision sensor is used to overcome the need of external technologies and runway knowledge. First-of-all, an existing structure of observation is applied to real landing scenarios; in this case, an observability analysis highlights some limitations of this solution. Therefore, a new extended observer solution is proposed which removes observability singularities. Last but not least, all simulation results have been obtained on an *Airbus* simulator used for certification purpose.

Keywords: pose estimation, nonlinear observer, aircraft landing.

1. INTRODUCTION

Automatic landing of a transport aircraft is possible thanks to external information. Most of the time, a ground system attached to the airport is needed, *e.g.* using the most common technology named *ILS* (Instrument Landing System). Thanks to this system, the deviations of the aircraft *w.r.t.* the runway can be computed and used in the guidance laws. However, this system is expensive and not available everywhere; furthermore, it requires additional procedures in air-traffic control. In frame of the future aircraft, manufacturers like *Airbus* study the possibility to make aircraft landing everywhere without information from ground external systems (unequipped or unknown runway). This paper is positioned within this framework.
The aircraft is assumed to be placed nearby the landing area with rough deviation thanks to current navigation technology (*GPS*, *IRS* (Inertial Reference System) or *VOR-DME* (VHF Omnidirectional Range/Distance Measuring Equipment). However, these systems are not precise/available enough to land on a runway. In parallel, Image Processing and camera technology have made a technological leap in the last decade. Hence, the use of a camera to perform visual servoing becomes an interesting solution to cope with precision and availability requirements.
This paper considers a generic runway whose size, position and markers are not known: geometric reconstruction solutions using these informations can not then be applied. However, thanks to IRS sensors, good accuracy and availability of aircraft motions and attitude can be considered. In this case, the use of the visual features motions between several images is sufficient to estimate deviations of the aircraft *w.r.t.* the runway. Afterwards, vision is only used to cope with relative position informations.
During landing, the estimated deviations can be used as output feedback in order to guide the aircraft (Gibert and Puyou (2013),Coutard and Chaumette (2011), Le Bras et al. (2009)) or as input in fusion sensor scheme. Note that image processing is a critical point for detection, tracking and extraction of features. The used algorithms (*e.g.* Schertler (2014)) are not discussed in this paper but results can be considered available.

Estimation of the deviations between a camera and a 3D point with a single embedded camera has been proposed in several range identification methods as in Karagiannis and Astolfi (2005), Dahl et al. (2005). The principle is that the estimator, initialized with a rough value, converges to one of the deviations of the camera *w.r.t.* a targeted point. Nevertheless, the system under consideration in the previous range identification methods does not provide sufficient observability features in conventional landing.
The present work proposes a new scheme for the relative pose estimation that guarantees observability improving estimation robustness to uncertainties *w.r.t.* previous approaches, and keeps simplicity.
A pose estimator inspired by Karagiannis and Astolfi (2005) has been implemented to highlight the estimation problem with a lack of observability during landing scenarios. This observer has been also extended to fit with the proposed system formulation.
Throughout this paper, all the simulations are made on an *Airbus* simulator used for certification purposes. The simulations are performed on a nonlinear model used for extensive clearance of the flight control laws. This model provides a very realistic behaviour of the aircraft and includes nonlinear characteristics of the main components: flight dynamics, flight control computer, actuators and sensors.
The paper is organized as follows. In Section 2, context of

the study is presented. Section 3 analyses an existing pose estimation method (Karagiannis and Astolfi (2005)) and propose an observability analysis along aircraft landings. Next, an extended observer is proposed in Section 4 with a simplified problem formulation, by using adequate visual features (Gibert and Puyou (2013)). This observer removes observability singularities and provide robustness to velocities uncertainties. Finally, Section 5 concludes this paper.

2. PROBLEM STATEMENT

The problem under interest consists in using a monocular camera embedded on a civil aircraft in order to overcome the need of external systems during an automatic landing. The single useful informations come from IRS and camera, IRS providing orientation and velocities whereas camera is providing visual features obtained from Image Processing. The main goal is to estimate deviations of the aircraft *w.r.t.* the runway. Then, these deviations could feed guidance laws algorithms.
In final approach, the desired trajectory, named glide path, is ending on the runway at a 3D point **E** attached to the inertial frame ($\mathcal{F}_i$) (see Figure 1). In this paper, the missing informations which need to be estimated are the deviations $\Delta_{X,Y,H}$ (Figure 1), expressed in the inertial frame ($\mathcal{F}_i$), of the aircraft *w.r.t.* **E** and the heading difference Δ_ψ between the runway and the aircraft. An other interesting deviation used is Δ_{GS}, which is the vertical deviation between the aircraft and the *Glide Slope*.

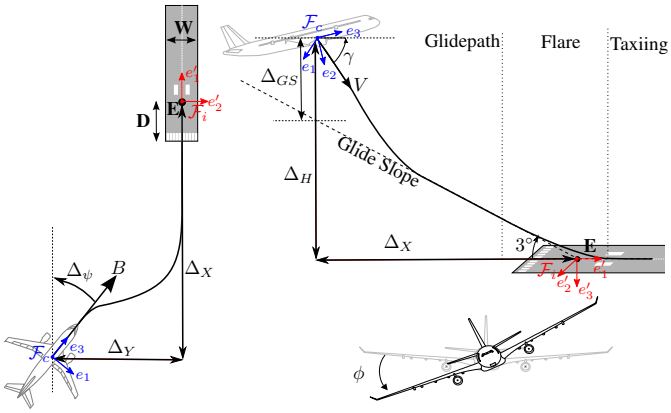

Fig. 1. Notations used in landing phase.

Thanks to external systems, one can consider that the aircraft is reaching a zone closed to the landing area. From this rough initial position, vision scheme is used to accurately estimate the deviations.
Three landing scenarios are proposed, each of them being characterized by three initial positions of the aircraft *w.r.t.* to the runway. Table 1 defines these three proposed initial positions; note that they correspond to an increasing difficulty (easy, medium, difficult) in term of dynamics of the aircraft.

Table 1. Initial conditions for landing scenarios

	Δ_X	Δ_Y	Δ_{GS}	ϕ	γ	Δ_ψ
Landing 1	$-5000m$	$+200m$	$-50m$	$0°$	$-3°$	$15°$
Landing 2	$-5000m$	$-200m$	$+50m$	$0°$	$-3°$	$0°$
Landing 3	$-4000m$	$400m$	$+100m$	$0°$	$-3°$	$-15°$

Throughout this paper, three trajectories of the aircraft (see Figure 2), from the initial conditions of Table 1, are used for the estimation study. These trajectories, obtained on the *Airbus* highly representative simulator, correspond to realistic behavior of aircraft in landing conditions.

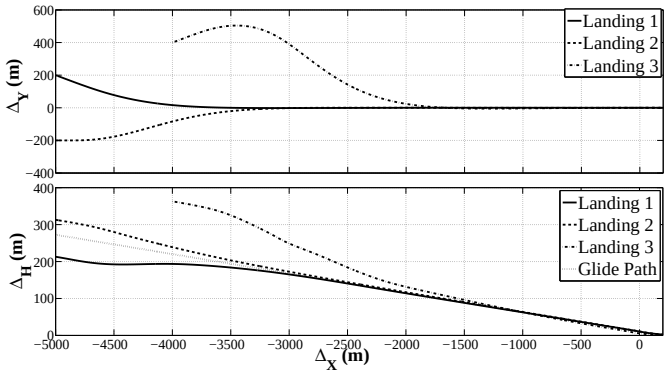

Fig. 2. Landings trajectories for three different scenarios.

Note that the aircraft presents a saturated vertical behavior ($\gamma > -6$) in Landing 3 which leads to a poorer glide tracking than other landings.

3. POSE ESTIMATION WITH STANDARD FORMULATION

3.1 Standard formulation

Consider the point **E**, a 3D point attached to the runway. This point could be expressed in the camera frame [1] ($\mathcal{F}_c$) and denoted $\mathbf{E}_c = [X_1\ X_2\ X_3]^T$. As proposed in Karagiannis and Astolfi (2005), the 3D-motion of $\mathbf{E}_c$ is

$$\dot{\mathbf{E}}_c = \underbrace{\begin{bmatrix} a_{11}(t) & a_{12}(t) & a_{13}(t) \\ a_{21}(t) & a_{22}(t) & a_{23}(t) \\ a_{31}(t) & a_{32}(t) & a_{33}(t) \end{bmatrix}_c}_{\mathbf{A}_c} \mathbf{E}_c + \underbrace{\begin{bmatrix} b_1(t) \\ b_2(t) \\ b_3(t) \end{bmatrix}_c}_{\mathbf{B}_c} \tag{1}$$

with $\mathbf{A}_c$ and $\mathbf{B}_c$ respectively angular and linear velocities matrices. For a civil aircraft, current inertial sensors technology allows to know motion parameters a_{ij} and b_i.

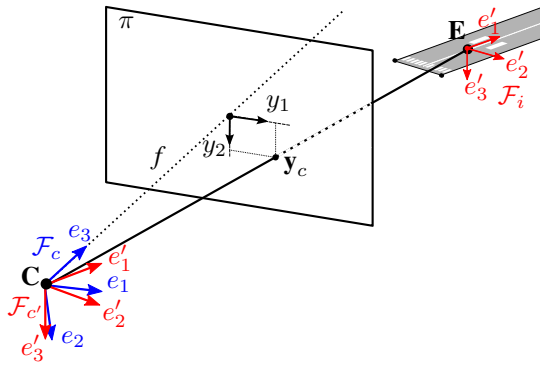

Fig. 3. Perspective projection of $\mathbf{E}_c$ in the image plane (π).

Given that $\mathbf{E}_c$ is not directly available, the single available information is the perspective projection $\mathbf{y}_c$ of $\mathbf{E}_c$ in the image plane (π) (see Figure 3) which reads as

$$\mathbf{y}_c = \begin{bmatrix} y_1 \\ y_2 \end{bmatrix}_c = f \begin{bmatrix} \frac{X_1}{X_3} & \frac{X_2}{X_3} \end{bmatrix}_c^T. \tag{2}$$

[1] A fixed camera is used; here, the aircraft frame can be supposed merging with it.

with f the known focal length of the camera.

In order to estimate X_1, X_2 and X_3 from $\mathbf{y}_c$, an observer can be applied on the system (1)-(2). Several observer have been proposed for this estimation problem. In this paper, the estimator from Karagiannis and Astolfi (2005) has been choosen because it appears to be one of the best candidates for its performances and its simplicity (reduced order observer).

3.2 Observer design

Following the notation of Karagiannis and Astolfi (2005), let $\eta \in \mathbb{R}$, the unmeasurable variable, define as

$$\eta = \frac{1}{X_3}. \tag{3}$$

System (1)-(2) is written in the ($\mathbf{y}_c$,η) coordinates, *i.e.*,

$$\begin{aligned} \dot{\mathbf{y}}_c &= \begin{bmatrix} a_{11}-a_{33} & a_{12} \\ a_{21} & a_{22}-a_{33} \end{bmatrix} \mathbf{y}_c + \begin{bmatrix} a_{13} \\ a_{23} \end{bmatrix} \\ &\quad -\mathbf{y}_c \mathbf{y}_c^T \begin{bmatrix} a_{31} \\ a_{32} \end{bmatrix} + \begin{bmatrix} b_1 - b_3 y_1 \\ b_2 - b_3 y_2 \end{bmatrix} \eta \\ \dot{\eta} &= -(a_{31}y_1 + a_{32}y_2 + a_{33})\eta - b_3\eta^2 \end{aligned} \tag{4}$$

Note that, when η is known, the coordinates $\mathbf{E}_c$ are easily obtained from (2), hence a reduced asymptottic observer of the state η is proposed. The dynamics of η read as

$$\dot{\hat{\eta}} = \alpha(\mathbf{y}_c, \hat{\eta}, t) \tag{5}$$

with $\mathbf{y}_c$ provided by (2). Define the error variable z as

$$z = \hat{\eta} - \eta + \beta(\mathbf{y}_c, t). \tag{6}$$

One gets

$$\dot{z} = \alpha - \dot{\eta} + \frac{\partial \beta}{\partial t} + \left[\frac{\partial \beta}{\partial \mathbf{y}_c}\right]^T \dot{\mathbf{y}}_c \tag{7}$$

The methodology proposed in Karagiannis and Astolfi (2005) consists in finding two *adequate* functions $\alpha(\cdot)$ and $\beta(\cdot)$ such that z converges to zero. Then, an asymptotic estimation $\bar{\eta}$ of the variable η reads as

$$\bar{\eta} = \hat{\eta} + \beta(\mathbf{y}_c, t). \tag{8}$$

Proposition 1. (Karagiannis and Astolfi (2005)). Consider the system (4) for which inequality

$$(b_1 - b_3 y_1)^2 + (b_2 - b_3 y_2)^2 > \delta > 0 \tag{9}$$

holds for all the landing scenarios, *i.e.* the system is observable. Then, given a known function $\alpha(\cdot)$, there exists a function $\beta(\mathbf{y}_c, t)$ such that the system (7) has an uniformly semi-globally asymptotically stable equilibrium at $z = 0$. ■

Proposition 2. An estimation of the state vector $\mathbf{E}$ of (1), denoted $[\hat{X}_1\ \hat{X}_2\ \hat{X}_3]^T$, reads as

$$\hat{X}_1 = \frac{y_1}{f \cdot \bar{\eta}}\ ,\ \hat{X}_2 = \frac{y_2}{f \cdot \bar{\eta}} \text{ and } \hat{X}_3 = \frac{1}{\bar{\eta}}. \tag{10}$$

with $\bar{\eta}$ defined by the reduced observer (5), (8). ■

Finally, the required information for the guidance control is the estimated vector $[\hat{\Delta}_X\ \hat{\Delta}_Y\ \hat{\Delta}_H]^T$ expressed in the inertial frame. From the estimated coordinates of $\mathbf{E}$ (10), it reads as

$$\begin{bmatrix} \hat{\Delta}_X \\ \hat{\Delta}_Y \\ \hat{\Delta}_H \\ 1 \end{bmatrix}_i = \begin{bmatrix} {}^c\mathcal{R}_i & {}^c\mathcal{T}_i \\ 0 & 1 \end{bmatrix} \begin{bmatrix} \hat{X}_1 \\ \hat{X}_2 \\ \hat{X}_3 \\ 1 \end{bmatrix}_c \tag{11}$$

with ${}^c\mathcal{R}_i$ and ${}^c\mathcal{T}_i$ the known rotation and translation matrices between the camera frame ($\mathcal{F}_c$) and the inertial frame ($\mathcal{F}_i$).

3.3 Observability analysis on landing scenarios

Before applying the previous observer, it is necessary to evaluate the observability during the landing scenarios.

As defined in the Proposition 1, the observability of system (1)-(2) is fulfilled if the inequality (9) is respected.

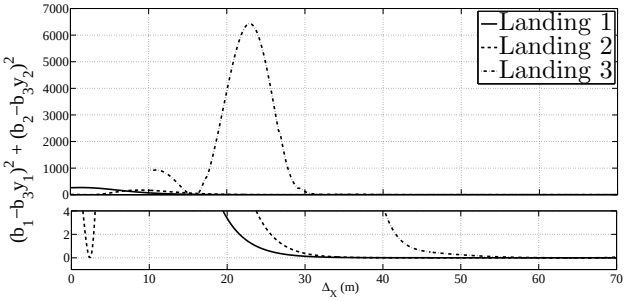

Fig. 4. Evolution of the left hand side of (9) along the 3 landings scenarios versus $\Delta_X(m)$ (**Top**: global behavior - **Bottom**: zoom around 0.)

Figure 4 displays the evolution of the left hand side of the inequality (9) throughout the 3 landings scenarios previously defined. The observability condition is satisfied during the "capture" of the glide path phase [2] ; however, observability is lost when the aircraft is aligned with the runway and on the glide path trajectory. Indeed, when the aircraft is laterally aligned with the runway, the output y_1 is in the middle of the image (*i.e.* $y_1 = 0$) and lateral velocity is null so $(b_1 - b_3 y_1) = 0$. Moreover, when the aircraft is tracking the glide path, output $y_2 = \tan(-3°)$ is corresponding to $\gamma = -3°$ (Gibert and Puyou (2013)) then $(b_2 - b_3 y_2) = 0$. In other words, when the aircraft is tracking the reference (*i.e.* performs a conventional landing), the left inside term of (9) is not strictly positive, hence the system is unobservable.

Remark 1. As written, the loss of observability occurs when the aircraft is aligned with the runway. If guidance algorithms based on estimation results are able to align the aircraft with respect to the runway, then the observability condition will be lost. This loss makes estimation potentially diverging; consequently, the guidance will shift the aircraft which brings back the observability, the control starting again to be efficient. Nevertheless, this behavior is not acceptable in an industrial context. ■

Observability analysis shows the existence of observability singularities. Given that these latter appears in non critical configurations (*i.e.* when the aircraft is on the glide path). Estimation is not ensured to converge which justify the use of an "extended"

[2] "Capture the glide path" means that the aircraft is reaching this desired trajectory. This phase is ending when the aircraft starts to track the glide path.

version of it.

4. AN IMPROVED OBSERVER SOLUTION

As viewed in the previous section, the choice of the visual features is a key point to guarantee observability. In the sequel, a new set of visual features is used to ensure a fair observability during all the landing phases. Thanks to these new visual features, a new extended observer based on Karagiannis and Astolfi (2005) is proposed.

4.1 New visual features

The coordinates of the point $\mathbf{E}$ in the image has been chosen because it is directly the aiming point (*i.e.* the reference) for a guidance point of view. Nevertheless, previous section has shown a lack of observability when using this point. A solution to provide observability all over the landing phase consists in using other points in the image.
Actually, every other point will provide observability during the alignment phase. An observer could then provide the relative pose of the aircraft with this other point. However, this other point will not correspond to the guidance reference and will certainly go outside of the image. The proposed points are the corners of the runway $\mathbf{L}$ and $\mathbf{R}$ (see Figure 5) which are attached to the runway and linked with the guidance reference $\mathbf{E}$. Considering that image processing algorithms are able to

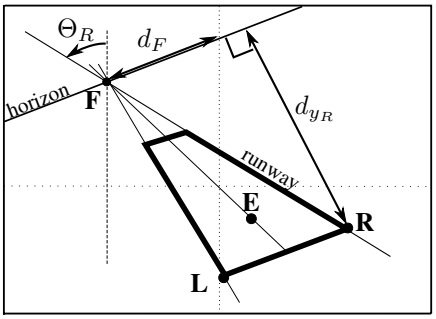

Fig. 5. Visual features Θ_R, d_F and d_{y_R}, the bold quadrilateral representing the runway.

detect the edges of the runway, it is possible to determine the coordinates in the image of $\mathbf{L}$ and $\mathbf{R}$; the measurement vector (2) becomes

$$\begin{bmatrix}\mathbf{y}_{c_L}\\ \mathbf{y}_{c_R}\end{bmatrix}_c = f\begin{bmatrix}\frac{X_{1_L}}{X_{3_L}} & \frac{X_{2_L}}{X_{3_L}} & \frac{X_{1_R}}{X_{3_R}} & \frac{X_{2_R}}{X_{3_R}}\end{bmatrix}_c^T. \tag{12}$$

Using the two points $\mathbf{L}$ and $\mathbf{R}$, the denominators in (12) (*i.e.* X_{3_L} and X_{3_R}) are not the same. Hence, it is not possible to defined the unmeasurable variable η of the previous observer. With visual features manipulations, it is possible to obtain a same denominator for the four elements of the measurement vector. Actually, it remains to express the problem in the inertial frame orientation. Thereafter, a way to obtain a common denominator in output vector is proposed.

4.2 Expression of the measurement in the inertial frame

Consider a new virtual frame $\mathcal{F}_{c'} = (C, e'_1, e'_2, e'_3)$ with the same center of the camera frame ($\mathcal{F}_c$) and with the orientation of inertial frame ($\mathcal{F}_i$). The 3D points $\mathbf{L}$ and $\mathbf{R}$ expressed in the virtual frame $\mathcal{F}_{c'}$ are denoted $\mathbf{L}_{c'}$ and $\mathbf{R}_{c'}$ (with $\mathbf{L}_{c'} = [X'_{1_L}\ X'_{2_L}\ X'_{3_L}]^T$ and $\mathbf{R}_{c'} = [X'_{1_R}\ X'_{2_R}\ X'_{3_R}]^T$).

Instead of using the output vector based on coordinates in the camera frame $\mathcal{F}_c$, this section explains how the measurement vector could be expressed with coordinates in the virtual frame $\mathcal{F}_{c'}$. Indeed, the measurement vector using $\mathbf{L}_{c'}$ and $\mathbf{R}_{c'}$ has the particularity to have the same denominator. With a similar structure than (12), a new output vector $\mathbf{y}_{c'}$ reads as

$$\mathbf{y}_{c'} = \begin{bmatrix}y_{1L}\\ y_{2L}\\ y_{1R}\\ y_{2R}\end{bmatrix}_{c'} = f\begin{bmatrix}\frac{X'_{1_L}}{X'_{3_L}} & \frac{X'_{2_L}}{X'_{3_L}} & \frac{X'_{1_R}}{X'_{3_R}} & \frac{X'_{2_R}}{X'_{3_R}}\end{bmatrix}_{c'}^T. \tag{13}$$

The new formulation of the output vector is obtained thanks to an adequate choice of visual features.

First visual feature.
The first visual feature d_F (see Figure 5) is the distance between the vanishing point $\mathbf{F}$ and the middle of the image along the horizontal line. The coordinates of $\mathbf{F}$ in the image is provided by image processing edges detection and corresponds to the intersection of the side lines [3]. d_F is used to compute the heading difference between the aircraft and the runway Δ_ψ. Actually, from the expression of d_F ((Gibert and Puyou, 2013)

$$d_F = f\Big(\frac{\tan\Delta_\psi}{\cos\theta} + \tan\phi\tan\theta\Big), \tag{14}$$

Δ_ψ can be easily computed through (15) using the measurement of d_F, the focal length f and angles θ and ϕ which are known.

$$\Delta_\psi = \tan^{-1}\Big(\cos\theta\Big(\frac{d_F}{f} - \tan\phi\tan\theta\Big)\Big) \tag{15}$$

Second and third visual features
Firstly, consider the point $\mathbf{R}$. Two additional visual features Θ_R and d_{y_R} (Figure 5) are used. Θ_R is the angle between the right sideline of the runway and the vertical of the camera frame and d_{yR} is the distance between R and the horizontal line. From the expression of $\mathbf{R}$ and $\mathbf{F}$ in the camera frame [4], the expression of the visual features Θ_R and d_{y_R} could be found with simple geometrical computations. It gives

$$\tan(\Theta_R) = \frac{\cos\phi\cos\theta X'_{2_R} - (\sin\phi\cos\Delta_\psi - \cos\phi\sin\Delta_\psi\sin\theta)X'_{3_R}}{\sin\phi\cos\theta X'_{2_R} + (\cos\phi\cos\Delta_\psi - \sin\phi\sin\Delta_\psi\sin\theta)X'_{3_R}} \tag{16}$$

$$d_{y_R} = f\frac{X'_{3_R}}{\cos\Delta_\psi\cos^2\theta X'_{1_R} - \sin\Delta_\psi\cos^2\theta X'_{2_R} + \cos\theta\sin\theta X'_{3_R}} \tag{17}$$

Recalling that the *IRS* informations are available, *i.e.* the pitch angle θ and the roll angle ϕ are known, and given Δ_ψ (15), a direct link between visual features Θ_R and d_{y_R} and relative deviation *w.r.t.* $\mathbf{R}$ in the virtual frame ($\mathcal{F}_{c'}$), *i.e.* X'_{1_R}, X'_{2_R} and X'_{3_R}, can be established.
Equations (16)-(17) can be written in order to express the relative pose of the aircraft depending on the visual features measurement. It gives

[3] Another solution could be to use the image processing algorithm from Schertler (2014) which provides the centreline of the runway. Then, it allows easily computing the vanishing point coordinates considering the horizontal line known (thanks to IRS measurements).

[4] The coordinates of $\mathbf{F}$ and $\mathbf{R}$, expressed in the camera frame $\mathcal{F}_c$, could be linked with the coordinates of $\mathbf{F}$ expressed in the inertial frame. Actually $F_c = {}^i\mathcal{T}_c F_i$ and $R_c = {}^i\mathcal{T}_c F_i$ with ${}^i\mathcal{T}_c$ the transformation matrix from $\mathcal{F}_i$ to $\mathcal{F}_c$.

$$\frac{X'_{1_R}}{X'_{3_R}} = \frac{1}{\cos\Delta_\psi \cos^2\theta}(f d_{y_R} + \sin\Delta_\psi \cos^2\theta \frac{X'_{2_R}}{X'_{3_R}} - \cos\theta\sin\theta)$$

$$\frac{X'_{2_R}}{X'_{3_R}} = \frac{1}{\cos\phi\cos\theta - \tan\Theta\sin\phi\cos\theta}(\tan\Theta\cos\phi\cos\Delta_\psi - \sin\phi\sin\Delta_\psi\sin\theta) + \sin\phi\cos\Delta_\psi - \cos\phi\sin\Delta_\psi\sin\theta). \quad (18)$$

By a similar way, considering the left corner point **L**, a virtual perspective projection

$$\frac{X'_{1_L}}{X'_{3_L}} \text{ and } \frac{X'_{2_L}}{X'_{3_L}} \quad (19)$$

could be expressed depending on its visual features Θ_L and d_{y_L}.

To summarize, informations derived from measured coordinates of **L** and **R** in the image and visual features properties give (18) and (19),which are the elements of (13). Given that the four elements of $\mathbf{y}_{c'}$ have similar denominator, it is possible to use it in the same framework of Karagiannis and Astolfi (2005) (ie to define η).

Note that the deviations X'_{2_L} and X'_{2_R} can be expressed depending on X'_{2_E} (with $\mathbf{E}_{c'} = [X'_{1_E}\ X'_{2_E}\ X'_{3_E}]^T$), X'_{2_E} being the lateral deviation of E in the virtual frame ($\mathcal{F}_{c'}$). One has

$$X'_{2_L} = X'_{2_E} - \frac{W}{2} \text{ and } X'_{2_R} = X'_{2_E} + \frac{W}{2} \quad (20)$$

with W the unknown width of the runway. Furthermore, X'_{2_E} which is

$$X'_{2_E} = \frac{1}{2}\left(X'_{2_L} + X'_{2_R}\right) \quad (21)$$

can be computed without knowing the runway width.

Note also that, in the virtual frame ($\mathcal{F}_{c'}$), $X'_{1_L} = X'_{1_R}$ and $X'_{3_L} = X'_{3_R} = X'_{3_E}$ (with a flat runway). The last information missing for guidance is X'_{1_L} which reads as

$$X'_{1_E} = X'_{1_L} + D \text{ or } X'_{1_E} = X'_{1_R} \quad (22)$$

with D a constant known distance between the ending point of the glide path **E** and the threshold of the runway.

As a consequence, system (1) can be written in the virtual camera frame ($\mathcal{F}_{c'}$) and is greatly simplified. It yields

$$\dot{\mathbf{E}}_{c'} = \mathbf{A}_{\mathbf{c}'}\mathbf{E}_{\mathbf{c}'} + \mathbf{B}_{\mathbf{c}'} \quad (23)$$

with $\mathbf{A}_{\mathbf{c}'} = \mathbf{0}$, and $\mathbf{B}_{\mathbf{c}'}$ the aircraft velocity vector in the virtual camera frame ($\mathcal{F}_{c'}$) which is the same of in inertial frame coordinates ($\mathcal{F}_i$) Consider the variable $\eta' = 1/X'_{3_E}$; then, from (23) and (13), consider the following system [5]

$$\begin{aligned} \dot{\eta}' &= -b'_3\eta'^2 \\ \dot{\mathbf{y}}_{c'} &= \begin{bmatrix} \dot{y}_{1L} \\ \dot{y}_{2L} \\ \dot{y}_{1R} \\ \dot{y}_{2R} \end{bmatrix}_{c'} = \eta' \begin{bmatrix} b'_1 - b'_3 y_{1L} \\ b'_2 - b'_3 y_{2L} \\ b'_1 - b'_3 y_{1R} \\ b'_2 - b'_3 y_{2R} \end{bmatrix}_{c'} \end{aligned} \quad (24)$$

for which $[\eta'\ \mathbf{y}_{c'}^T]^T$ is the state variable whose only the part $\mathbf{y}_{c'}$ is measured.

[5] The simplicity of the system (24) compared with (4) comes from the formulation of the problem in the virtual frame $\mathcal{F}_{c'}$.

In order to analyze the observability of (24)-(13), consider the following Jacobian matrix Φ

$$\Phi = \begin{bmatrix} 1 & 0 & 0 & 0 \\ 0 & 1 & 0 & 0 \\ 0 & 0 & 1 & 0 \\ * & * & * & b'_1 - b'_3 y_{1L} \\ * & * & * & b'_2 - b'_3 y_{2L} \\ * & * & * & b'_1 - b'_3 y_{1R} \\ * & * & * & b'_2 - b'_3 y_{2R} \end{bmatrix} \quad (25)$$

with $\omega = [y_{1L}\ y_{2L}\ y_{1R}\ y_{2R}\ \eta]^T$ and $*$ denoting terms with no impact on the observability.

Proposition 3. (Krener and Respondek (1985)). System (24) with the measurement vector (13) is observable if the rank of (25) is full, *i.e.* $Rank(\Phi) = 4$. ■

From the previous proposition, it yields that observability condition is fulfilled if

$$(b'_1 - b'_3 y_{1L})^2 + (b'_2 - b'_3 y_{2L})^2 + (b'_1 - b'_3 y_{1R})^2 + (b'_2 - b'_3 y_{2R})^2 > 0 \quad (26)$$

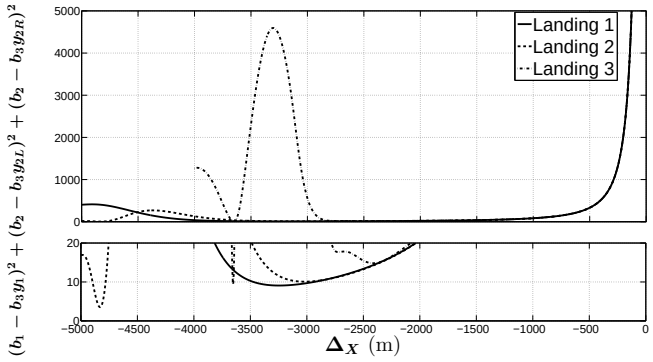

Fig. 6. Evolution of the left hand side of (26) along the 3 landings scenarios versus Δ_X (m) (**Top**: global behavior - **Bottom**: zoom around 0.)

Figure 6 displays the left hand side of the inequality (26) throughout the 3 landings scenarios. It appears that the observability condition (26) is fulfilled all along the landing phase. In fact, from (26), one can remark that, with $b'_3 \neq 0$, $b'_2 - b'_3 y_{2L}$ and $b'_2 - b'_3 y_{2R}$ could not be equal to zero at the same time. Indeed, $y_{2L} = X'_{2_E} - \frac{W}{2}$ is different from $y_{2R} = X'_{2_E} + \frac{W}{2}$. If $b'_3 = 0$, the aircraft is flying levelled; however b'_1 is never null in fixed wing vehicle conventional landing. Then, the observability condition is always guaranteed for system (24) and (13).

4.3 Extended Observer design

By using new visual features and geometrical properties, a new measurement vector (13) has been obtained. Nevertheless, the design of observer propose in section 3 does not accept a output vector with four elements. In the sequel, an observer is proposed for system (13)-(24) and can be viewed as an extension of Karagiannis and Astolfi (2005) given that the dimensions of the state and output vectors are greater.

Proposition 4. An estimation of the state vector $\mathbf{E}_{\mathbf{c}'}$ of system (23), denoted $[\hat{X}'_{1_E}\ \hat{X}'_{2_E}\ \hat{X}'_{3_E}]^T$ reads as

$$\begin{aligned}\hat{X}'_{1_E} &= \frac{\hat{X}'_{3_E} \cdot \frac{y_{1L}+y_{1R}}{2}}{f} \\ \hat{X}'_{2_E} &= \frac{\hat{\Delta}_H \cdot (y_{2L}+y_{2R})}{2f} \\ \hat{X}'_{3_E} &= \frac{1}{\bar{\eta}'}\end{aligned} \tag{27}$$

with $\bar{\eta}'$ defined by the reduced observer

$$\dot{\hat{\eta}} = \alpha(\mathbf{y}_{c'}, \hat{\eta}, t) \ \text{ and } \ \bar{\eta} = \hat{\eta} + \beta(\mathbf{y}_{c'}, t) \tag{28}$$

with

$$\begin{aligned}\alpha(\mathbf{y}_{c'}, \hat{\eta}, t) &= \left[\frac{\partial \beta}{\partial \mathbf{y}_{c'}}\right]^T \begin{bmatrix} b'_1 - b'_3 y_{1L} \\ b'_2 - b'_3 y_{2L} \\ b'_1 - b'_3 y_{1R} \\ b'_2 - b'_3 y_{2R} \end{bmatrix} (\hat{\eta} + \beta(\mathbf{y}_{c'}, t)) \\ &\quad - \frac{\partial \beta}{\partial t} - b'_3 (\hat{\eta} + \beta(\mathbf{y}_{c'}, t))^2, \\ \beta(\mathbf{y}, t) &= \frac{\lambda}{2}\Big((-y_{1L}^2 - y_{2L}^2 - y_{1R}^2 - y_{2R}^2) b'_3 \\ &\quad + 2b'_1 (y_{1L} + y_{1R}) + 2b'_2 (y_{2L} + y_{2R}) \Big).\end{aligned} \tag{29}$$

■

Sketch of proof. Given the functions $\alpha(\cdot)$ and $\beta(\cdot)$ (29), the proof of Proposition 4 is based on a similar way than the initial observer of Karagiannis and Astolfi (2005).

4.4 Simulation results

Results obtained for the three defined landings in presence of biased velocities are presented in Figure 7. The conditions of

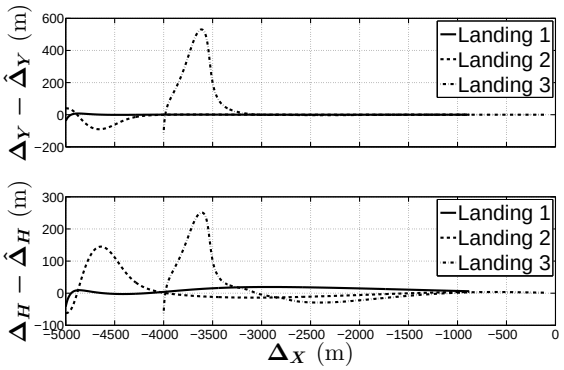

Fig. 7. Error between lateral (Δ_Y) and longitudinal (Δ_H) deviations and its estimates ($\hat{\Delta}_Y$ and $\hat{\Delta}_H$) in presence of bias on velocities measurement, with respect to Δ_X.

simulation are strictly the same as previously (in particular, same bias on the velocities provided by IRS).
Contrary to the previous results, the errors between the deviations and their estimated values reach and are maintained at zero. In fact, given that the observability condition is respected along the landing phases, the observer is able to correct estimation till convergence.

5. CONCLUSION AND FUTURE PERSPECTIVES

This paper has proposed a relative pose estimation solution for automatic landings of civil aircraft with a reduced number of informations coming from external means. After using an adequate set of visual features in order to simplify the problem formulation, a nonlinear observer has been applied on a landing scenario. An extended solution of this observer has been proposed in order to guarantee observability and convergence of the estimation all over the landing. All the observation solutions have been evaluated on *Airbus* simulator used for certification purpose.
Future works will focus on the effect of estimation in guidance performances. Indeed, the estimation overshoot in presence of bias on velocities could produce a non desired behaviour in close loop. Noise, calibrations errors and delay caused by Image Processing will be explored. Moreover, a complete landing estimation solution will be performed to handle the problem of losing the corners in the image (Burlion and de Plinval (2013)). We also would like to try to extend our observability analysis as well as our estimation scheme while using other visual features e.g lines / visual moments (Chaumette (2004)).

REFERENCES

Burlion, L. and de Plinval, H. (2013). Keeping a ground point in the camera field of view of a landing uav. In *IEEE International Conference on Robotics and Automation (ICRA)*.

Chaumette, F. (2004). Image moments: a general and useful set of features for visual servoing. *IEEE Transactions on Robotics*, 20(4), 713–723.

Coutard, L. and Chaumette, F. (2011). Visual detection and 3d model-based tracking for landing on an aircraft carrier. In *IEEE International Conference on Robotics and Automation*. Shanghai, China.

Dahl, O., Nyberg, F., Holst, J., and Heyden, A. (2005). Linear design of a nonlinear observer for perspective systems. In *IEEE International Conference on Robotics and Automation (ICRA)*. Barcelona, Spain.

Gibert, V. and Puyou, G. (2013). Landing of a transport aircraft using image based visual servoing. In *9th IFAC Symposium on Nonlinear Control Systems (NOLCOS)*. Toulouse, France.

Karagiannis, D. and Astolfi, A. (2005). A new solution to the problem of range identification in perspective vision systems. *IEEE Transactions on Automatic Control*, 50(12), 2074–2077.

Krener, A.J. and Respondek, W. (1985). Nonlinear observers with linearizable error dynamics. *SIAM Journal on Control and Optimization*, 23(2), 197–216.

Le Bras, F., Hamel, T., Barat, C., and Mahony, R. (2009). Nonlinear image-based visual servo controller for automatic landing guidance of a fixed-wing aircraft. In *European Control Conference*. Budapest, Hungary.

Schertler, K. (2014). Method and device for image-assisted runway localization, patent n. wo.2014.075657, germany.